Journal of Applied Sciences

ISSN 1812-5654

science alert

ANSInet
an open access publisher
http://ansinet.com

Journal of Applied Sciences 9 (21): 3857-3863, 2009
ISSN 1812-5654

FDTD Method Including Material Dispersion for Solution of Fundamental Space-Filling Mode in Photonic Crystal Fibers

[1]A. Pourkazemi, [1]M. Mansourabadi and [2]A. Kashaninia
[1]Faculty of Electrical Engineering, K.N. Toosi University of Technology Tehran, Islamic Republic of Iran
[2]IAUCTB, Tehran, Iran

Abstract: In this study, a Finite-Difference Time-Domain (FDTD) method including material dispersion for the full-vectorial analysis of Fundamental Space-filling Mode (FSM) of photonic crystal fibers is presented and we examine four different methods based on FDTD, to calculate FSM of a fiber to present the best possible method to solve a cladding structure. In order to improve the accuracy of results obtained by this method, we propose an initial field distribution, apply Padé approximation technique and employ a constitutive-parameter averaging technique. We also investigate the influence of the accuracy of the solution on the Effective Index Method (EIM) which is based on FDTD via comparing the effective index and chromatic dispersion results obtained by both FDTD and FDTD Effective Index Methods (FDTD-EIM). To use the effective index method in order to calculate the effective index, we implement different equivalent radii and the most suitable radius is introduced among them. In conclusion, we show that by using known equivalent radii, FDTD-EIM is not able to provide reasonable results.

Key words: Effective index method, dispersion, Padé approximation, conformal technique, initial field distribution

INTRODUCTION

In recent years, Photonic Crystals Fibers (PCFs) have attracted much attention due to some extraordinary properties, such as wide single-mode wavelength range, unusual chromatic dispersion and high or low non-linearity (Saitoh and Koshiba, 2005). Because of these properties, PCFs have found applications in various optical fields, such as nonlinear optics (Ranka *et al*., 2000; Bowden and Zheltikov, 2002), ultrafast science (Reeves *et al*., 2003) optical metrology (Udem *et al*., 2002), nonlinear spectroscopy (Konorov *et al*., 2004) and microscopy (Paulsen *et al*., 2003), biomedical optics (Hartl *et al*., 2001) and optical sensing (Myaing *et al*., 2003).

Index-guiding PCFs are usually formed by a central solid defect region surrounded by multiple air holes of wavelength-scale in a regular hexagonal array running along the entire fiber length (Li *et al*., 2004). Different modeling methods have been introduced to study the characteristics of PCFs, including the plane wave expansion method (Ferrando *et al*., 1999), the Effective-Index Method (EIM) (Knight *et al*., 1998), the finite-difference method in the time domain (FDTD) (Qiu, 2001) or frequency domain (FDFD) (Zhu and Brown, 2002) and the finite element method (FEM) (Brechet *et al*., 2000). Among these methods, the FDTD method using Yee's mesh (Yee, 1966) has been successfully applied to PCFs and is much easier to implement while it can obtain acceptable accuracy. A compact two-dimensional (2-D) scheme is usually used to compute guided modes in PCFs if one assumes that the propagation constant along the z-direction (propagation direction) is fixed (Qiu, 2001; Choi and Hoeffer, 1986; Asi and Shafai, 1992). Thus, it is possible to obtain the effective index (n_{eff}) from PCF formed by a defect surrounded by circular air holes in hexagonal lattice.

The Fundamental Space-filling Mode (FSM) of a PCF is defined as the mode with the largest modal index of the infinite two-dimensional photonic crystal that constitutes the PCF cladding (Bjarklev *et al*., 2003; Birks *et al*., 1997). Finding FSM of a PCF yields the effective cladding index (n_{FSM}).

Once having the effective cladding index and effective index, it is possible to calculate confinement loss (Koshiba and Saitoh, 2005), bending loss (Nielsen *et al*., 2004), splice loss and effective modal spot size (Kliros *et al*., 2006) and also to determine single-mode region (Birks *et al*., 1997).

Corresponding Author: Ali Pourkazemi, Faculty of Electrical Engineering, K.N. Toosi University of Technology, Seyedkhandan, P.O. Box 16315-1355, Dr. Shariati Ave, Tehran, Islamic Republic of Iran
Tel: +98 9126611085 Fax: +98 21 88462066

As well, this study presents a FDTD-based method for solving the FSM of PCFs. The influence of the solution accuracy on the EIM is investigated via comparing n_{eff} and dispersion results obtained by FDTD and FDTD Effective Index Method (FDTD-EIM). Using Auxiliary Differential Equation (ADE) technique (Taflove, 1995) and considering the frequency dependence of the material refractive index in this study, we have achieved more accurate numerical results. However, to improve accuracy and convergence, we use an averaging method which is based on conformal technique.

To facilitate obtaining effective cladding index and the effective index and to increase the accuracy of the algorithm, we introduce a specific initial field distribution and apply Padé approximation technique (Dey and Mittra, 1998). All simulations are written in C++ language and run on a PC with Intel 2.41 GHz processor and 512 MB memory.

NUMERICAL METHODS

FDTD algorithm: For a linear isotropic material in a source-free region, the time-dependent Maxwell's equations can be written as:

$$\nabla \times \vec{E} = -\mu(r)\frac{\partial \vec{H}}{\partial t} \quad (1)$$

$$\nabla \times \vec{H} = \varepsilon(r)\frac{\partial \vec{E}}{\partial t} + \sigma(r)\vec{E} + \vec{J} \quad (2)$$

where, $\mu(r)$, $\varepsilon(r)$ and $\sigma(r)$ are the position-dependent permeability, permittivity and conductivity of the material, respectively. $\vec{J}$ is the polarization current density in the material induced by the electric field and is used to model dispersive materials in FDTD method. However, it is considered zero in non-dispersive materials.

According to Yee-cell technique, Maxwell's equations can be discretized in space and time on a discrete three-dimensional mesh (Qiu, 2001). Assuming that the fields of the guided modes in PCFs depend on $\exp(-j\beta_z z)$ (β_z is the propagation constant) along the propagation direction, the z-derivatives in Maxwell's equations can be replaced by $-j\beta_z$ and only reexpressed in terms of the transverse variables.

To avoid complex number computations, it is possible to assume that the TE field components (H_x, H_y, E_z) are composed of the $\cos(\beta_z z+\varphi)$ and the TM field components (E_x, E_y, H_z) are composed of the $\sin(\beta_z z+\varphi)$, rather than complex exponentials, so the resulting equations will be solved faster with less required memory, while the accuracy will remain the same (Qiu, 2001). The algorithm stability is guaranteed as long as the time increment (Δt) satisfies:

$$\Delta t \le 1/c\sqrt{2\Delta h^{-2}+(\beta_z/2)^2}$$

where, c is the speed of the light and $\Delta h = \Delta x = \Delta y$ are dimensions of unit cell of 2-D mesh (Qiu, 2001).

Inclusion of dispersion: To include material dispersion, we use the ADE formulation which is employed for multiple Lorentz pole pairs in (Taflove, 1995) and Sellmeire's formula that nicely fits the wavelength dependence of the refractive index of the fused silica. However, by optimizing the effective constitutive parameters for fused silica, it is possible to simplify Sellmeire's formula to two resonant frequencies without losing accuracy in the wavelength range of interest for PCFs (0.5-2.0 μm) (Wei *et al*., 2006). This simplification can efficiently decrease the computation time and memory while the results are accurate in the mentioned range.

Boundary condition: To solve an FSM problem, it is possible to apply Yee's algorithm to a unit cell that acts like a boundless propagation medium. Figure 1 shows the unit cell of cladding structure.

By tiling the structure shown in Fig. 1 infinitely, it is possible to present the infinite two-dimensional photonic crystal; this will be possible, by applying appropriate boundary conditions at each four sides of structure. Considering the unit cell along with the Periodic Boundary Conditions (PBCs) expressed as (Taflove, 1995):

$$\vec{E}_x\big|_{i=0} = \vec{E}_x\big|_{i=i_{max}} e^{j\beta_x L_x} \quad (3)$$

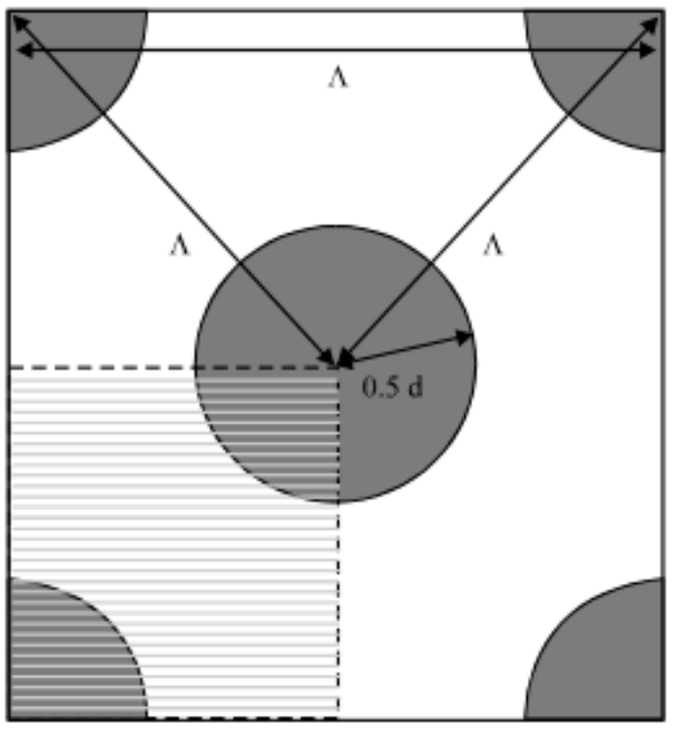

Fig. 1: The unit cell of cladding used to solve FSM problem; the reduced unit cell is surrounded by dashed line

$$\breve{E}_x\Big|_{i=i_{max}+1} = \breve{E}_x\Big|_{i=1} e^{-jk_x L_x} \quad (4)$$

the unit cell can be set to act like 2-D infinite photonic crystal that constitutes the PCF cladding structure. Note that Eq. 3 and 4 are written along x for E_x and other boundary conditions can be derived according to Taflove (1995).

The 2-D photonic crystal unit cell of interest spans from FDTD grid cell (0, 0) and (0, j_{max}) to (i_{max}, 0) and (i_{max}, j_{max}). On the other hand, the FDTD formulation (Qiu, 2001) is not able to calculate the x-component of electric fields at the first column grid points (i = 0, j), thus it is enough to copy the fields at the last column grid points (i = i_{max}, j) to those at the first column grid points according to Eq. 3. We are merely interested in effective index of the infinite photonic crystal cladding, so we can reduce Eq. 3 to 5:

$$E_x^n\Big|_{j=0} = E_x^n\Big|_{j=j_{max}} \quad (5)$$

which is definitely simpler and faster than Eq. 3 and 4. The following equations are obtained for the other field components in the same way:

$$E_y^n\Big|_{i=0} = E_y^n\Big|_{i=i_{max}} \quad (6a)$$

$$E_z^n\Big|_{i=0} = E_z^n\Big|_{i=i_{max}} \quad (6b)$$

$$E_z^n\Big|_{j=0} = E_z^n\Big|_{j=j_{max}} \quad (6c)$$

$$H_x^n\Big|_{j=j_{max}} = H_x^n\Big|_{j=0} \quad (7a)$$

$$H_y^n\Big|_{i=i_{max}} = H_y^n\Big|_{i=0} \quad (7b)$$

$$H_z^n\Big|_{i=i_{max}} = H_z^n\Big|_{i=0} \quad (7c)$$

$$H_z^n\Big|_{j=j_{max}} = H_z^n\Big|_{j=0} \quad (7d)$$

Note that Eq. 5 to 6c should be applied after electric fields calculation while Eq. 7a-d are applied after magnetic fields calculation.

An alternative unit cell that is simpler and faster to implement is surrounded by dashed line in Fig. 1. For setting the reduced unit cell to act like cladding structure, the periodic boundary conditions Eq. 5-7 change to:

$$E_y^n\Big|_{j=0} = E_y^n\Big|_{j=j_{max}} = E_y^n\Big|_{i=0} = E_y^n\Big|_{i=i_{max}} = E_z^n\Big|_{i=0} = E_z^n\Big|_{i=i_{max}} = 0 \quad (8)$$

$$H_x^n\Big|_{i=0} = H_x^n\Big|_{i=i_{max}} = H_x^n\Big|_{j=0} = H_x^n\Big|_{j=j_{max}} = H_z^n\Big|_{j=0} = H_z^n\Big|_{j=j_{max}=0} \quad (9)$$

Excitation: Point-wise source or artificial random initial field distribution can be used to excite the structure (Taflove, 1995; Qiu and He, 2000). However, due to the experiences, we found out that after the steady state is reached, the first mode will be dominant if initial field distribution introduced in the FDTD algorithm is approximately the same as field distribution of the first mode. This scheme has two important advantages in PCF simulations. First, it can reduce the total number of the time steps to reach steady state and second, the detection of the first mode is easier and more accurate. Assuming that the center of unit cell is located at ($1/2j_{max}$, $1/2i_{max}$), we use the following relation to initialize *y*-component of magnetic field.

$$H_y^0 = \exp\left(-\frac{i-0.5\times i_{max}}{\alpha\times i_{max}}\right)\times\exp\left(-\frac{j-0.5\times j_{max}}{\beta\times j_{max}}\right) \quad (10)$$

By trial and error, we found optimized value of 1.3 for α and β.

Padé approximation and conformal technique: The accuracy of FFT results is dependent on the total number of time steps, which means a larger number of time steps leads to more accurate result by FDTD. Thus we use Padé approximation technique (FFT/Padé) reported by Dey and Mittra (1998), to efficiently increase the accuracy of FFT results obtained by simulation.

In order to have significantly improved numerical stability and accuracy, it is possible to use effective values of the constitutive parameters which are simply given by a weighted area average of the material constitutive parameters on each side of the medium interface.

To apply this technique, it is enough to substitute the constitutive parameters with the effective constitutive parameters in polarization current updating equations. This technique is the same as that used in the plane expansion method (Johnson and Joannopoulos, 2001), FDTD (Dey and Mittra, 1999) and FDFD (Zhu and Brown, 2002).

Method verification: To verify our method numerically, we study the fundamental space-filling mode formed by a hexagonal lattice of circular air holes in silica (Fig. 1) and applying Eq. 5-7. The lattice pitch is 2.3 μm and the diameter of the air holes is d = 1 μm. Taking the time increment $\Delta t = 0.1/c\sqrt{2\Delta h^{-2} + \beta_z^2/4}$ and the total number of time steps 2^{15}, we let a space increment of $\Delta h = 20/\Lambda$ and $\Lambda/50$. Table 1 contains numerical results at λ = 1 and 1.55 μm for different analysis types while it also depicts the results obtained by FEM to provide comparison

Table 1: Cladding index and simulation time by different types

	Method*				
	1	2	3	4	FEM
λ = 1 μm	1.43339	1.42723	1.42517	1.42288	1.42994
Δh = Λ./20	20.609 sec	20.820 sec	666.954 sec	4.657 sec	
λ = 1 μm	1.43157	1.42877	1.42506	1.42723	
Δh = Λ./50	293.532 sec	296.824 sec	4234.172 sec	62.578 sec	
λ = 1.55 μm	1.41057	1.40354	1.37362	1.39683	1.40836
Δh = Λ./20					
λ = 1.55 μm	1.40448	1.40457	1.36931	1.40207	
Δh = Λ./50					

*Method 1: Original Unit Cell, without FFT/Padé, no Conformal, using the method (Taflove, 1995), Method 2: Original unit cell, with FFT/Padé, Conformal, using the method (Taflove, 1995), Method 3: Original unit cell, with FFT/Padé, Conformal, using the method (Wei *et al*., 2006), Method 4: Reduced unit cell, with FFT/Padé, Conformal, using the method (Taflove, 1995)

between different results (Brechet *et al*., 2000). Another alternative to include material dispersion was introduced by Wei *et al*. (2006). However, their method involves complex numbers in calculation, thus it does not lead to result as fast as the method used in this study. The fourth column in Table 1 is considered to illustrate the analysis by the method of Wei *et al*. (2006).

Studying Table 1 significantly suggests that using FFT/Padé and effective constitutive parameter techniques improves the numerical results and gives closer answer to FEM in comparison with all of the methods introduced by Taflove (1995).

Table 1 shows that the results achieved by method 3 are not close to FEM as much as those by method 2. Besides, method 3 takes more time to run because of using complex numbers (due to present simulations, method 2 was at least up to 33 times faster than method 3). So, it is logical to use the method of Taflove (1995) in the rest of this study.

Another useful result from Table 1 is that although using reduced unit cell is faster than using original unit cell, the results obtained by it deviate from the results obtained by FEM. This can be due to the fact that by tiling discretized reduced unit cells, the exact original cell is not produced. However, to get closer to the exact original unit cell, it is possible to tile discretized reduced unit cell with smaller Δh. In this case, the obtained result may get closer to FEM.

From Table 1, it is obvious that as the Δh decreases, the obtained results get closer to that obtained by FEM so that by setting Δh = Λ/100 the cladding index at λ = 1 and 1.55 μm will be 1.42951 and 1.40572, respectively. In the rest of this paper, we let Δh = Λ/100.

RESULTS

Figure 2a and b show the patterns of the x- and y-components of the electric field of the fundamental mode for λ = 1 μm, Λ = 2.3 μm and d/Λ = 0.43.

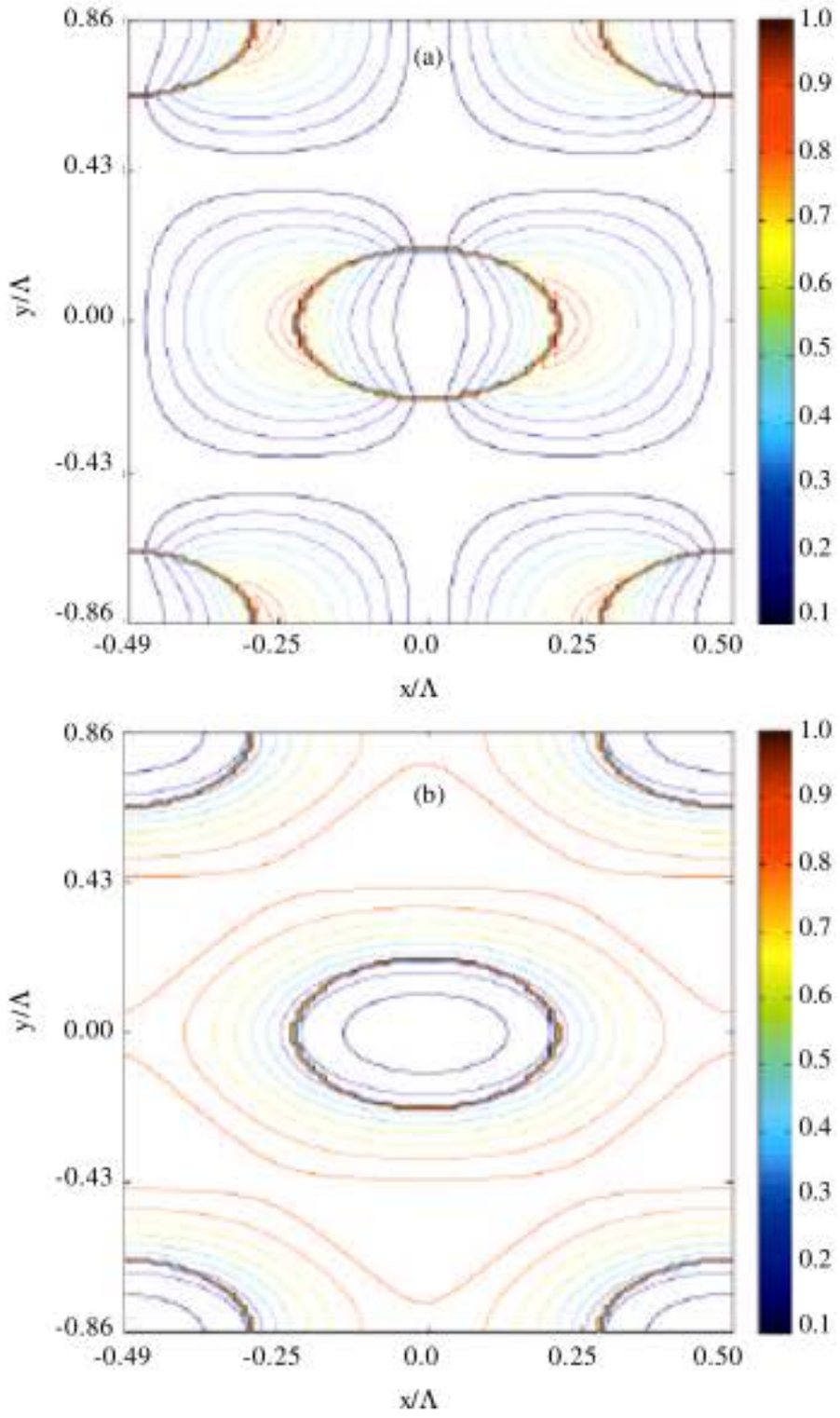

Fig. 2: Contour plots of the transverse electric-field components of the fundamental mode in the cladding for Λ = 2.3 μm and d/Λ = 0.43 at λ = 1 μm (a) z-component of the electric field and (b) y-component of the magnetic field

Figure 2 can help to choose the best possible initial field distribution for FDTD algorithm. However, by studying Fig. 2, it is understood that achieving an analytical and simple function to present the field distribution approximately, is not that easy. Equation 10 proved to be a very good function to produce initial field for both cladding and photonic crystal fiber structures, Though field distribution by using Eq. 10 can not present the obtained fields in Fig. 2.

Assuming Λ = 1 μm and d/Λ= 0.4, 0.6 and 0.8, the cladding effective indices obtained by FDTD is shown in Fig. 3.

Based on EI methods, once having effective cladding index, it is possible to solve the characteristic equation of the step-index fiber to obtain effective index

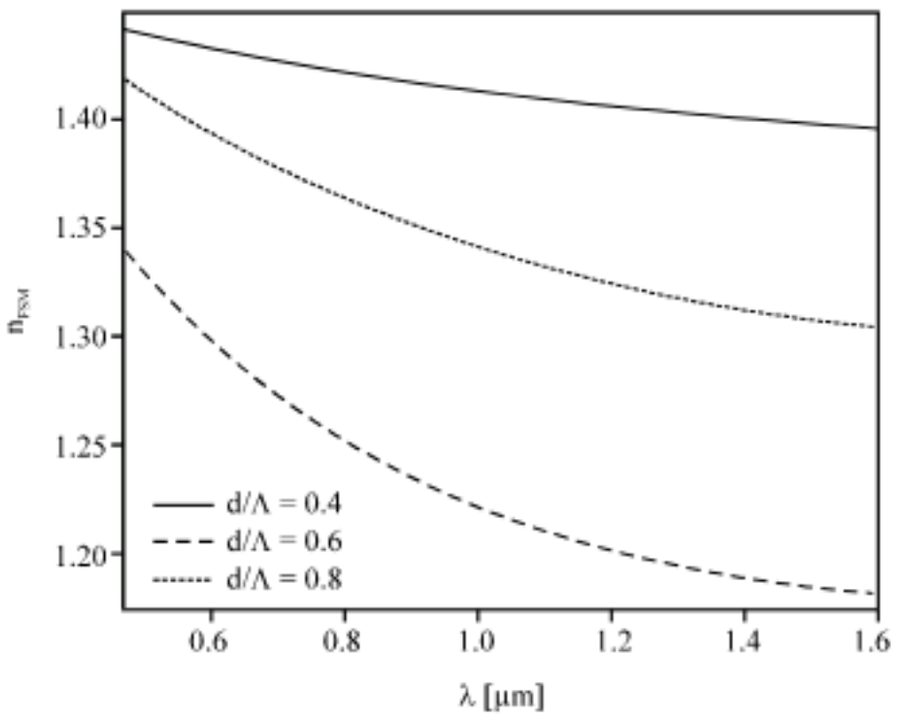

Fig. 3: The cladding effective index obtained by FDTD for $\Lambda = 1$ μm and $d/\Lambda = 0.4$, 0.6 and 0.8

(Li *et al*., 2004, 2006; Knight *et al*., 1998). To demonstrate the accuracy of this method, we compare the results of EIM which uses our FSM solver with those of FDTD method while analyzing a PCF structure. We calculate the effective index of mentioned PCF while taking the time increment $\Delta t = 0.1/c\sqrt{2\Delta h^{-2} + \beta_z^2/4}$, total number of time steps 2^{15} and space increment $\Delta h = \Lambda/20$. We use the Convolutional Perfectly Matched Layer (CPML) technique (Roden and Gedney, 2000) for the FDTD boundary treatment while the excitation is done by initial field distribution and the results are obtained by FFT/Padé.

When using EI methods, the effective radius of the equivalent step index fiber can significantly change the result. We used the same radii as used in various EIM calculations for evaluation of effective index (i.e., $R = \left(\sqrt{3}/2\pi\right)^{0.5}\Lambda$, $R = 0.5\Lambda$ and $R = 0.625\Lambda$ (Li *et al*., 2004). To compare the results for suggested radii, the absolute difference of effective index (for different effective radii) between that obtained by EIM-FDTD and FDTD is plotted in Fig. 4. It is obvious that for $d/\Lambda = 0.8$, the results obtained by EIM-FDTD, regardless of considered effective radius, deviate from the results obtained by FDTD (Fig. 4). In addition, the results do not suggest the best possible effective radius amongst the used effective radii.

Figure 4a-c clearly show that implementation of different radii can lead to various results, so using common radii for EIM-FDTD is not a good idea. Obviously by changing fiber parameters (d/Λ and Λ), the accuracy of obtained results changes dramatically. Because of dependence of accuracy on the effective radius, d/Λ and Λ, it is logical to apply a radius which is dependent on d/Λ and Λ, so that the accuracy of the method lay in a reasonable range.

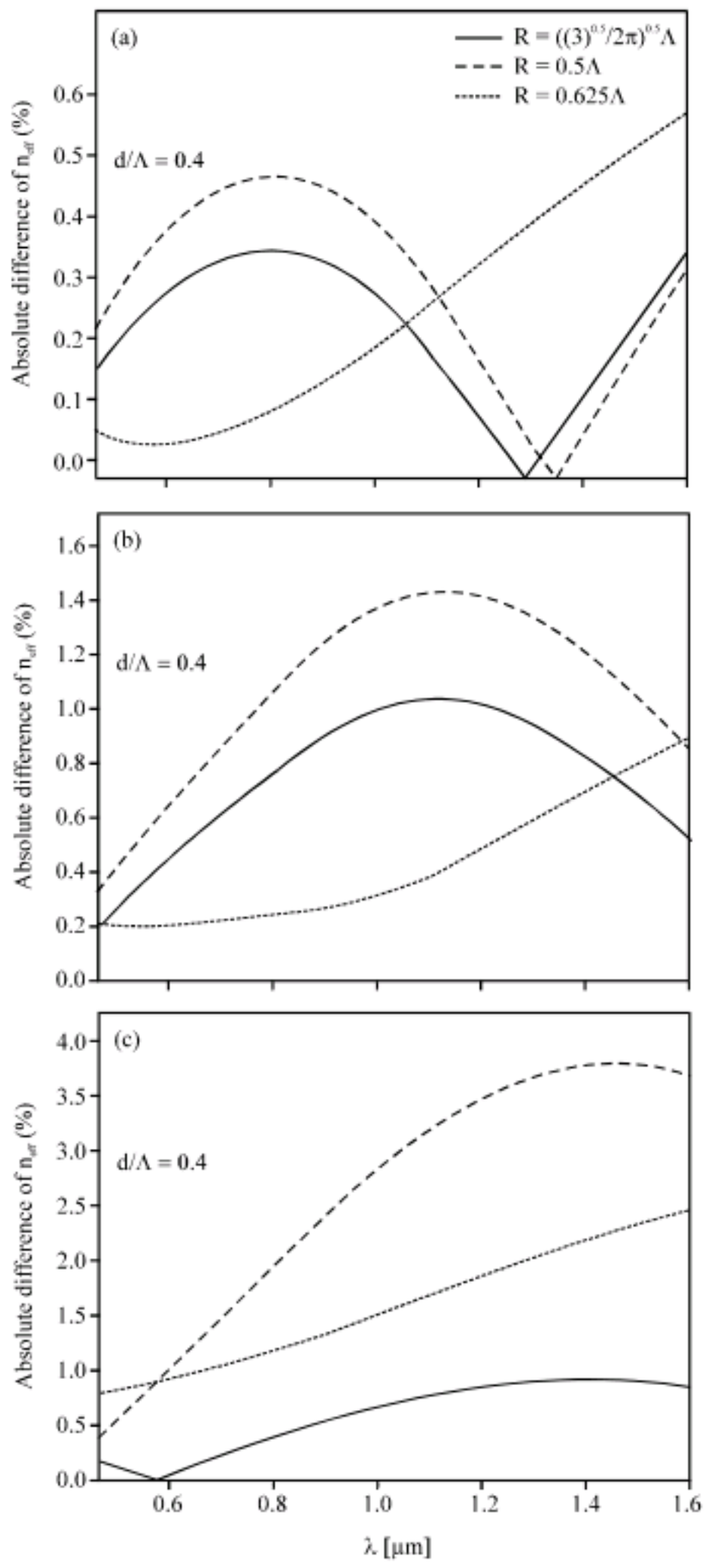

Fig. 4: Absolute difference between effective index of a PCF for $\Lambda = 1$ μm obtained by FDTD and FDTD-EIM using various effective radius (a) = 0.4, (b) = 0.6 and (c) = 0.8

Furthermore, to study the accuracy of the achieved solution based on FDTD-EIM, we calculate the chromatic dispersion of a PCF by FDTD and FDTD-EI methods (Fig. 5). For this comparison we let $R = 0.5\Lambda$, which results in the worst effective index over the wavelength for $d/\Lambda = 0.8$. Note that we purposely chose $R = 0.5\Lambda$ and

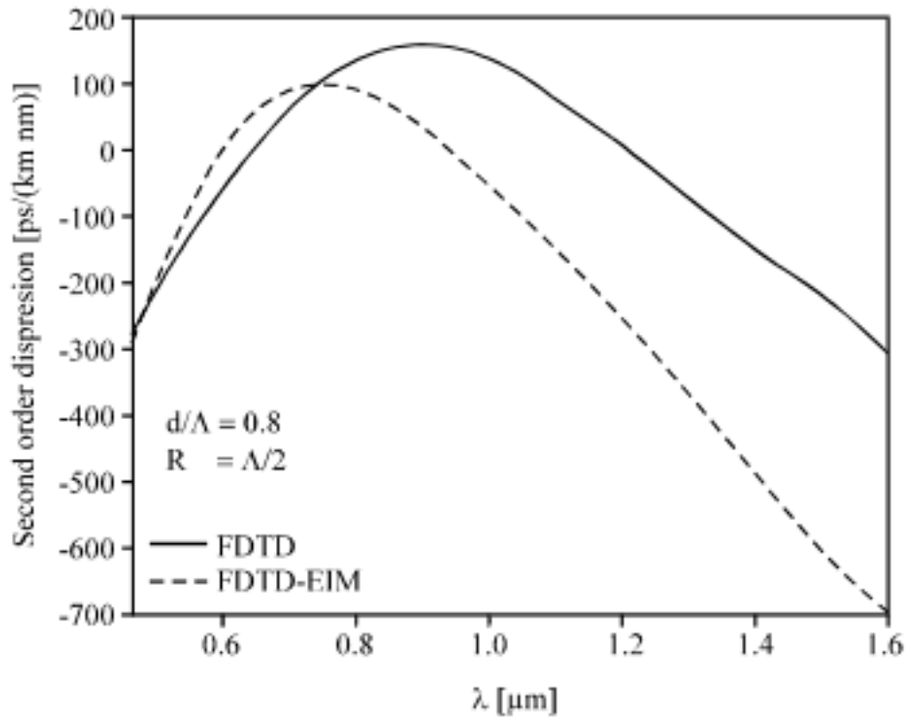

Fig. 5: Results obtained by FDTD and FDTD-EIM methods for $\Lambda = 1$ μm, $R = 0.5\Lambda$ and $d/\Lambda = 0.8$

$d/\Lambda = 0.8$ so that the dispersion curve indicates the maximum possible error among the obtained results.

According to Fig. 5, it is obvious that FDTD-EIM for $R = 0.5\Lambda$ and $d/\Lambda = 0.8$ obtains different results from FDTD method. At the wavelength of 1.6 μ, the relative error between two methods is about 133% which is clearly unacceptable. This result definitely suggests that using FDTD-EIM with common radii used in other effective index methods is not recommended. Moreover, it is clear that calculation of via solving the characteristic equation of the step-index fiber does not lead to reasonable results. As well, since the accuracy of effective index affects the accuracy of chromatic dispersion, employing the mentioned method and considering the mentioned effective radii are not recommended for calculating the dispersion in spite of the fact that the method is faster. Of course Mansourabadi and *et al*. (2009) showed that when dealing non-dispersive materials, FDTD-EIM by using common radii can lead to good results, but the obtained results show that in dispersive case, applying a new radius is necessary.

DISCUSSION

In this study, by incorporating a specific periodic boundary condition for compact-2-D FDTD method, we could present a method to solve the fundamental space-filling mode of a PCF with inclusion of material dispersion. In order to increase the accuracy of analysis of results obtained by simulation, we proposed an initial field distribution which also could reduce the total number of time steps needed to reach steady state. A technique called Padé approximation was used to both decrease the total number of time steps and increase the accuracy of algorithm while averaging constitutive parameters were employed to improve both accuracy and convergence. On the other hand, using the suggested algorithm avoids using complex numbers and this advantage significantly decreases the simulation time. With present FDTD fundamental space-filling mode solver, we numerically analyzed the effective cladding index of a typical PCF and demonstrated the validity of our method. The numerical results indicate that a reduced unit cell does not lead to accurate results unless the algorithm accuracy increases. Besides using a reduced unit cell, three other methods were examined and the results by these four methods clearly recommend different methods for different situations. So that when the cost and time is more important, it is advisable to implement reduced unit cell and when just the accuracy has higher priority, using complete unit cell with mentioned methods in the study is inevitable.

Based on EI methods, we calculated the effective index by using different equivalent step-index fiber radii and showed that the results obtained by using the mentioned radii do not lead to the accurate result. Though using common radii used in EI methods can obtain good results for non-dispersive case, our research shows that these radii are not suitable for dispersive problems. Then one can investigate the relation between different radii and accuracy and introduce a radius as the function of fiber parameters. In that case FDTD-EIM will be a strong method to solve effective index problems in both non-dispersive and dispersive problems.

REFERENCES

Asi, A. and L. Shafai, 1992. Dispersion analysis of anisotropic inhomogeneous waveguides using compact 2-D-FDTD. Electron. Lett., 28: 1451-1452.

Birks, T.A., J.C. Knight and P.S.J. Russell, 1997. Endlessly single-mode photonic crystal fiber. Opt. Lett., 22: 961-963.

Bjarklev, A., J. Broeng and A.S. Bjarklev, 2003. Photonic Crystal Fibres. Kluwer Academic, Boston.

Bowden, C.M. and A.M. Zheltikov, 2002. Nonlinear optics of photonic crystals. J. Opt. Soc. Am. B, 19: 2046-2048.

Brechet, F., J. Marcou, D. Pagnoux and P. Roy, 2000. Complete analysis of the characteristics of propagation into photonic crystal fibers by the finite element method. Opt. Fiber Technol., 6: 181-191.

Choi, D.H. and W.J.R. Hoeffer, 1986. The finite-difference time-domain method and its application to eigen-value problems. IEEE Trans. Micro. Theory Techniques, 34: 1464-1470.

Dey, S. and R. Mittra, 1998. Efficient computation of resonant frequencies and quality factors of cavities via a combination of the finite-difference time-domain technique and the Padé approximation. IEEE Micro. Guided Wave Lett., 8: 415-417.

Dey, S. and R. Mittra, 1999. A conformal finite-difference time-domain technique for modeling cylindrical dielectric resonators. IEEE Trans. Micro. Theory Techniques, 47: 1717-1739.

Ferrando, A., E. Silvestre, J.J. Miret, P. Andres and M.V. Andres, 1999. Fullvector analysis of a realistic photonic crystal fiber. Opt. Lett., 24: 276-278.

Hartl, I., X.D. Li, C. Chudoba, R.K. Rhanta and T.H. Ko *et al*., 2001. Ultrahigh-resolution optical coherence tomography using continuum generation in an air-silica microstructure optical fiber. Opt. Lett., 2: 608-610.

Johnson, S.G. and J.D. Joannopoulos, 2001. Block-iterative frequency-domain methods for Maxwell's equations in a planewave basis. Opt. Express, 8: 173-190.

Kliros, G.S., J. Konstantinidis and C. Thraskias, 2006. Prediction of macrobending and splice losses for photonic crystal fibers based on the effective index method. WSEAS Trans. Commun., 5: 1314-1321.

Knight, J.C., T.A. Birks, P.S.J. Russell and J.P. De-Sandro, 1998. Properties of photonic crystal fiber and the effective index model. J. Opt. Soc. Am. A, 15: 748-752.

Konorov, S.O., D.A. Akimov, E.E. Serebryannikov, A.A. Ivanov, M.V. Alfimov and A.M. Zheltikov, 2004. Cross-correlation FROG CARS with frequency-converting photonic-crystal fibers. Phys. Rev. E, 70: 057601-057604.

Koshiba, M. and K. Saitoh, 2005. Simple evaluation of confinement losses in holey fibers. Opt. Commun., 253: 95-98.

Li, Y., C. Wang and M. Hu, 2004. A fully vectorial effective index method for photonic crystal fibers: Application to dispersion calculation. Opt. Commun., 238: 29-33.

Li, Y., C. Wang, Y. Chen, M. Hu, B. Liu and L. Chai, 2006. Solution of the fundamental space filling mode of photonic crystal fibers: Numerical method versus analytical approaches. Applied Phys. B: Lasers Opt., 85: 597-601.

Mansourabadi, M., A. Poorkazemi, M. Shamloufard and Y. Riazi, 2009. Finite-difference time-domain method solution of fundamental space-filling mode in photonic crystal fibers. J. Applied Sci., 9: 2801-2807.

Myaing, M.T., J.Y. Ye, T.B. Norris, T. Thomas and J.R. Jr. Baker *et al*., 2003. Enhanced two-photon biosensing with double-clad photonic crystal fibers. Opt. Lett., 28: 1224-1226.

Nielsen, M., N. Mortensen, M. Albertsen, J. Folkenberg, A. Bjarklev and D. Bonacinni, 2004. Predicting macrobending loss for large-mode area photonic crystal fibers. Opt. Express, 12: 1775-1779.

Paulsen, H.N., K.M. Hilligse, J. Thøgersen, S.R. Keiding and J.J. Larsen, 2003. Coherent anti-Stokes Raman scattering microscopy with a photonic crystal fiber based light source. Opt. Lett., 28: 1123-1125.

Qiu, M. and S. He, 2000. Numerical method for computing defect modes in two-dimensional photonic crystals with dielectric or metallic inclusions. Condensed Matter Mater. Phys., 61: 12871-12876.

Qiu, M., 2001. Analysis of guided modes in photonic crystal fibers using the finite-difference time-domain method. Microw. Opt. Tech. Lett., 30: 327-330.

Ranka, J.K., R.S. Windeler and A.J. Stentz, 2000. Visible continuum generation in air-silica microstructure optical fibers with anomalous dispersion at 800 nm. Opt. Lett., 25: 25-27.

Reeves, W.H., D.V. Skryabin, F. Biancalana, J.C. Knight and P.S J. Russell *et al*., 2003. Transformation and control of ultra-short pulses in dispersion-engineered photonic crystal fibres. Nature, 424: 511-515.

Roden, J.A. and S.D. Gedney, 2000. Convolutional PML (CPML): An efficient FDTD implementation of the CFS-PML for arbitrary media. Microw. Opt. Technol. Lett., 27: 334-339.

Saitoh, K. and M. Koshiba, 2005. Empirical relations for simple design of photonic crystal fibers. Opt. Express, 13: 267-274.

Taflove, A., 1995. Computational Electrodynamics: The Finite-Difference Time-Domain Method. Artech House, Norwood, MA.

Udem, T., R. Holzwarth and T.W. Hänsch, 2002. Optical frequency metrology. Nature, 416: 233-237.

Wei, J., L. Shen, D. Chen and H. Chi, 2006. An extended FDTD method with inclusion of material dispersion for the full-vectorial analysis of photonic crystal fibers. J. Lightwave Technol., 24: 4417-4423.

Yee, K.S., 1966. Numerical solution of initial boundary value problems involving Maxwell's equations in isotropic media. IEEE Trans. Antennas Propag., 14: 302-307.

Zhu, Z. and T.G. Brown, 2002. Full-vectorial finite-difference analysis of microstructured optical fibers. Opt. Express, 10: 853-864.